NRC Publications Archive
Archives des publications du CNRC

Extracting Main Modes of Human Shape Variation from 3-D Anthropometric Data
Ben Azouz, Zouhour; Shu, Chang; Lepage, R.; Rioux, Marc

Publisher's version / Version de l'éditeur:

National Research
Council Canada

Conseil national
de recherches Canada

Institute for
Information Technology

Institut de technologie
de l'information

NRC·CNRC

*Extracting Main Modes of Human Shape Variation from 3-D Anthropometric Data ***

Ben Azouz, Z., Shu, C., Lepage, R., and Rioux, M.
June 2005

Canada

Extracting Main Modes of Human Body Shape Variation from 3-D Anthropometric Data

Zouhour Ben Azouz[1,2]   Chang Shu [1]   Richard Lepage [2]   Marc Rioux[1]

[1] *Visual Information Technology Group*
National Research Council of Canada
{*Zouhour.Benazouz, Chang.Shu, Marc.Rioux*}*@nrc-cnrc.gc.ca*

[2] *Département de génie de la production automatisée*
École de technologie supérieure de Montréal
Richard.Lepage@etsmtl.ca

Abstract

Characterizing the variations of the human body shape is fundamentally important to many applications ranging from animation to product design. 3-D scanning technology makes it possible to digitize the complete surfaces of a large number of human bodies, providing much richer information about the body shape than the traditional anthropometric measurements. This technology opens up opportunities to extract new measurements for quantifying the body shape. Using the data from the first large scale 3-D anthropometric survey, the CAESAR project, we demonstrate that the human body shape can be represented by a small number of principal components. Principal Component Analysis extracts orthogonal basis vectors, called eigenpersons, from the space of body shapes. The shape of any individual person can then be expressed by the linear combination of the basis vectors. We demonstrate that some of these components correspond to the commonly used body measurements like height and weight and others indicate new ways of charactering body shape variations. We develop tools to visualize the changes of the body shape along the main components. These tools help understand the meaningful components of the human body shape.

1   Introduction

The shape of the human body has complex geometry and varies from person to person. No two persons have exactly the same shape. On the other hand, all human bodies share a common structure regardless of age, race, and gender. How do we quantify human body shapes? What is a good representation of their variations? The answers to these questions have diverse applications in, for example, human systems engineering, computer animation, and medical care.

Traditionally, anthropometry—the study of human body measurement—characterizes human body with linear distances between anatomical landmarks or circumferences at predefined locations. While this is a compact description, they do not uniquely specify the shape of the human body. Furthermore, the measurement relies on manual operations that are inefficient and prone to errors.

3-D scanning technology makes it possible to digitize the complete surfaces of a large number of human bodies. CAESAR, which stands for Civilian American and European Surface Anthropometry Resource, is the first large scale 3-D anthropometry survey project [15]. About 6000 civilians, between the age of 18 and 65 in the USA, the Netherlands and Italy, were scanned in three postures wearing tight clothes and hair coverings. The Cyberware WB4 [8] and Vitronic [9] full-body scanners were used. A set of 74 white markers were also placed at anatomical landmarks prior to scanning.

The first attempt in processing 3-D anthropometric data for analyzing the body shape is to extract traditional anthropometric measurements from the scanned data [5]. Working with the 3-D surface data has the advantage of being able to perform repeated measurements without the subject being present.

The 3-D scans contain much more information about the human body shape than the traditional anthropometric measurements; they provide opportunities to extract new measurements for quantifying the body shape. Inspired by the work of characterizing the space of faces in 2-D im-

ages and 3-D scans using Principal Component Analysis (PCA) [4, 13], Ben Azouz et al. [2, 3] and Allen et al. [1] extract orthogonal basis vectors, called *eigenpersons*, from the space of body shapes. The shape of any individual person can be expressed by the linear combination of the basis vectors.

We have two purposes in this paper. First, we show that human body shape can be represented with a small number of principal components. Second, we show that some of these components correspond to commonly used body measurements like height and weight and others indicate new ways of charactering the body shape. We demonstrate that the intuitive meanings of these components are easily realized through visualizing the changes of the body shape along each main component. By interpreting the components, we provide insight into these new quantities, which may lead to more effective use of the shape variations in applications that need to compare, synthesize, recognize, and monitor human bodies.

2. Model representation

The central issue in applying the PCA to the 3-D anthropometric data is to bring all the models in correspondence to each other. Each model in the database contains around 300,000 triangles. Making a correspondence means all models under consideration have to be sampled with equal number of points and every point in one model has a unique matching point in every other model. One approach to establishing the correspondence is to fit a template mesh model to the scanned data [1, 16]. Anatomical landmarks are used for guiding the deformation of the template surfaces to fit the scanned data. Unfortunately, placing markers at the landmark locations is a difficult and time-consuming task that involves palpating the body prior to scanning. Thus, future anthropometric surveys will unlikely use landmarks.

In this paper we focus on human shape analysis without relying on anatomical landmarks. In a previous paper [3] we propose to establish a correspondence between different models by converting their surface meshes to a volumetric representation and analyzing how the same volume is occupied by different models. We then compute a signed distance field on the volumetric representation and use the distance function to perform the principal component analysis. This is similar to the 2-D face recognition approach [13]. As a consequence we do not require the anatomical landmarks.

The volumetric representation does not provide an exact correspondence, but our experiments show that it is adequate for characterizing the global body shape variations. We summarize the essential aspects of creating a volumetric representation in the next two subsections.

2.1 Preprocessing

Because of occlusions and low grazing angles, the models from the CAESAR database do not in general represent a closed surfaces; there are holes in them, as shown in Figure 1(a) and Figure 1(c). In order to compute an accurate distance field, it is necessary to repair these models. Several methods provide smooth hole-fillings for 3-D models [6, 7]. However, they are not adequate for repairing the CAESAR models because they can produce undesirable bridges between the two legs and in the areas under the arms, and bulbous shapes for the bottom of the feet.

Special model repairing techniques have been developed for fixing human models. Stralen et al. [18] developed a toolbox for identifying holes in 3-D human body scans. The basic idea is to detect and classify holes according to body segments. A potential use of the classification is to fit templates of body parts to missing areas. A library of body parts is then required. However, fitting these parts to missing data is not straightforward. The method proposed by Allen et al. [1] solves the hole-filling problem effectively by fitting a template surface, but this method relies on anatomical landmarks.

We propose to repair the CAESAR models by estimating the missing data from the measured information using a slicing method. A model is first sliced horizontally. For each slice, if the model is water-tight, it should consist of closed curves. Therefore, open curves in the slice indicate holes and the hole-filling amounts to properly bridging the boundary points of the open curves. We define a cost function based on the surface normals and the distances between each pair of the boundary points. We find the best pairing of the boundary points by minimizing the cost function. Once the best pairings are found, the open curves are closed by interpolating the boundary points with degree two Bézier curves. More details of the hole-filling process can be found in [3].

The CEASAR models suffer from severe lack of data on the hands. Since our goal is to analysis the global body shape, we segment out the hands in our experiments.

2.2 Voxelization

Voxelization is to embed a continuous surface representation of a geometric object in a regular grid. Early voxelization algorithms were binary, assigning 1 to the occupied voxels and 0 to the unoccupied ones [11, 12]. Models created by binary voxelization suffer from aliasing. One way to reduce the aliases is to apply low-pass filters to the voxels [12].Alternatively, distance field techniques, which assign each voxel the distance to its nearest surface point, can be used to solve the aliasing problem [10]. Despite requiring substantially more computation, we chose the dis-
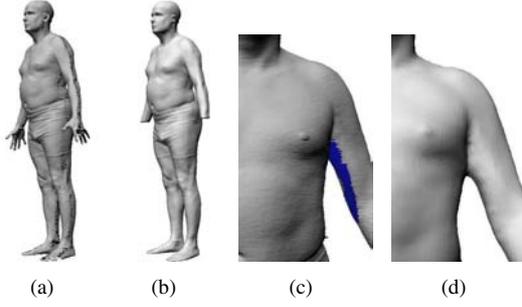
Figure 1. Repairing of a CAESAR human model. (a)&(c) Original model; (b)&(d) Repaired model.
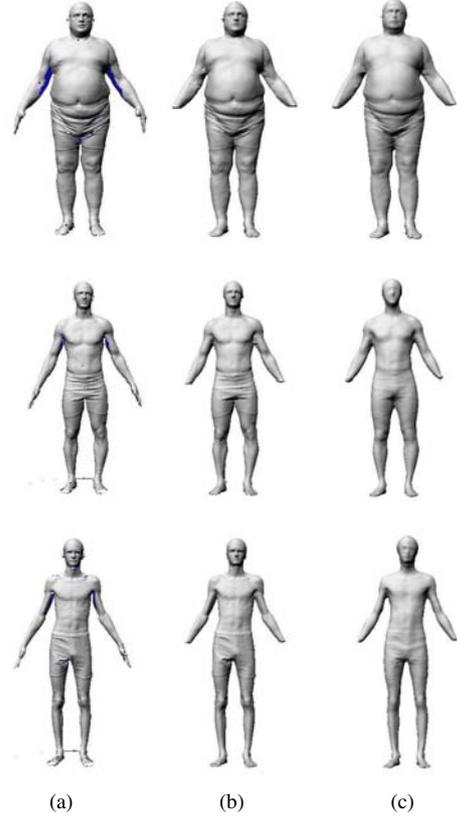

Figure 2. Reconstruction of human models using the first 64 eigenvectors extracted from the volumetric representation of 300 male subjects. (a) Original models; (b) Repaired models; (c) Reconstructed models.

tance field technique, because it gives a continuous distance function that is suitable for the principal component analysis.

3 Principal component analysis

To apply PCA to the volumetric models, we form a vector, $\boldsymbol{\Psi}$, for each model, where each element of the vector is the signed distance from a voxel to the surface of the model. The average over N models is given by $\bar{\boldsymbol{\Psi}} = (1/N)\sum_{i=1}^{N}\boldsymbol{\Psi}_i$. The deviation vectors $\boldsymbol{\Phi}_i = \boldsymbol{\Psi}_i - \bar{\boldsymbol{\Psi}}$ are arranged in a matrix $\mathbf{A} = [\boldsymbol{\Phi}_1 \boldsymbol{\Phi}_2 \cdots \boldsymbol{\Phi}_N]$. The PCA of the matrix $\mathbf{A}$ generates a set of non-correlated eigenvectors $\mathbf{u}_i$ and their corresponding variances λ_i. The eigenevectors are sorted according to the decreasing order of their variances. Each vector $\boldsymbol{\Phi}_i$ can be approximated as

$$\hat{\boldsymbol{\Phi}}_i \approx \sum_{j=1}^{M} c_{ij}\mathbf{u}_j, \tag{1}$$

where $0 \le M \le N$ and $c_{ij} = \boldsymbol{\Phi}_i \cdot \mathbf{u}_j$. In other words, every model can be reconstructed by the linear combination of a subset of the eigenvectors. The quality of the reconstruction can be evaluated by the fraction $\sum_{i=1}^{M}\lambda_i / \sum_{i=1}^{N}\lambda_i$, representing the percentage of the variance spanned by the eigenvectors chosen for the reconstruction.

4 Reconstruction

The principal component analysis is applied to 300 male subjects from the CAESAR database. Only the standing posture is considered in our experiments. The models are first converted to a volumetric representation. The PCA extracts a set of eigenvectors that represent an orthogonal basis of the human shape space inside the studied models. The eigenvectors are arranged according to the decreasing order

of the percentage of the shape variability that they induce. Experimental results show that the first 64 eigenvectors represent 95% of the total variance. Figure 2 illustrated three examples of the reconstructed models using Equation 1. For visualization purpose, we convert the volumetric models back to the surface meshes using the marching cube algorithm [14]. As we can see, even with reduced number of coefficients, the global geometry of the the reconstructed body shapes are fairly close to the original scans.

5 Interpretation of main modes of variation

The first few eigenvectors extracted by applying PCA to a set of human models represent the main modes of shape variation within the studied population. In this section we visualize the first five modes of variation and give interpretations of these modes, linking them to some intuitive body shape variations. This information is important for many

applications, for example, the design of products that inter-act with humans.

To visualize the main modes of the shape variation, we start from the projection of a real model onto the basis of main components. For each mode of variation, we generate a sequence of virtual models by changing the coefficient of correlation with the corresponding eigenvector, while keeping the rest of the coefficients constant. The sequence of virtual models show only the shape variation that is induced by the corresponding mode of variation. The interpretations of these modes are made obvious by animating the virtual models. Representative virtual models are presented and compared with the real models with the same range of coefficients.

We conducted three groups of experiments. In the first group, we apply PCA to the original models. In the second group, we normalize models to the same height before applying PCA. There are two reasons for the normalization. One is that it isolates the shape variation from the height variation. Another is that it improves the correspondences between the models, because if the models are at the same height, their anatomical components tend to align with each other better. After normalizing the height, the arms represent the body segments where the misalignment is the most severe and in some extreme examples one model's arm can correspond to part of another model's torso. These misalignments introduce artificial variabilities that do not reflect the changes of the body shape. Therefore, in the third group of experiments we eliminate the arms.

In the following interpretations we concentrate on the overall body shape variation and ignore the details on the heads. Our method can be applied to the heads separately. Tables 1 and 2 summarize the interpretations of the first five modes under non-normalized and normalized conditions respectively.

In 1940, Sheldon et al. [17] proposed three components for characterizing the human body: endomorphy (soft and roundness), mesomorphy (hardness and muscularity) and ectomorphy (linearity and skinniness). Our interpretations can be considered as a generalization of these components. While Sheldon et al.'s observations are qualitative, we provide quantitative measurements.

mode	interp.	variability
1st	weight & height	35.0%
2nd	$weight/(height)^3$	15.0%
3rd	alignment artifact	9.53%
4th	leaning posture	4.02%
5th	muscularity	3.17%

Table 1. Non-Normalized

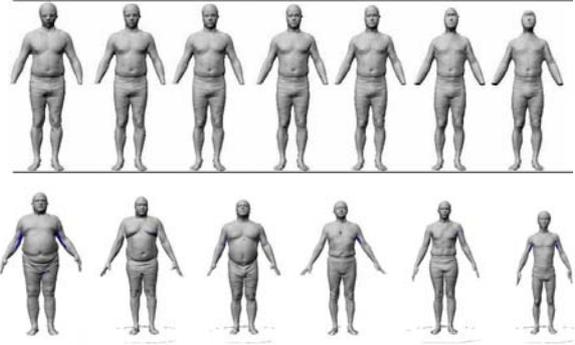| mode	interp.	variability
1st	weight	33.86%
2nd	leaning posture	15.11%
3rd	muscularity	8.93%
4th	arm-torso spacing	4.0%
5th	head position	3.64%

Table 2. Normalized

Figure 3. First mode of variation without height normalization (35.01% of the total shape variability). This mode represents a combination of height and weight variation. First row: virtual models; Second row: original models.

5.1 Non-normalized models

The modes of variation are presented in decreasing order of the percentage of the variability they induce.

5.1.1 First mode

The first mode of variation, representing 35% of the total shape variability within the studied set of models, reflects a combination of height and weight (but dominated by height). In Figure 3, we arrange models in increasing order of their projection on the first main component. One side of the mode represents tall and wide persons and the other side represents short and thin ones.

5.1.2 Second mode

The second mode of variation is highly correlated to the normalized weight, which we define as the ratio of the weight and the cube of the height. In Figure 4, each dot represents a model with the horizontal axis as the normalized weight and the vertical axis as the correlation with the second mode of variation. This mode of variation represents 15% of the global variance. Figure 5 shows that the models changes from thin on the left to wide on the right.
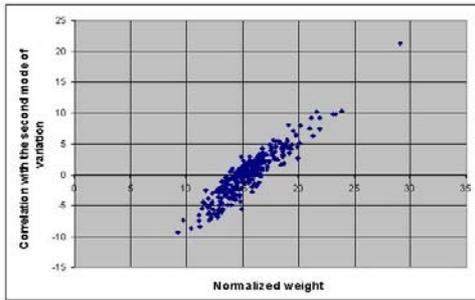
Figure 4. Correlation between the second mode of variation and the normalized weight.
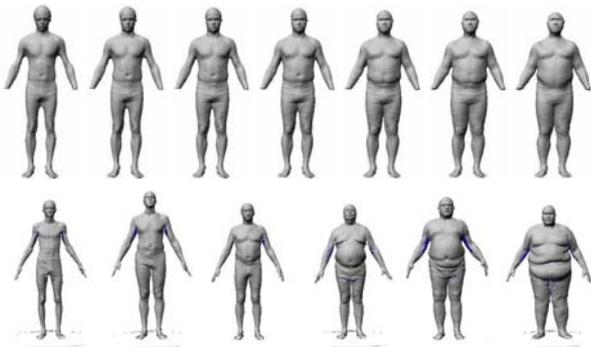

Figure 5. Second mode of variation without height normalization. This mode is correlated to the normalized weight ($weight/(height)^3$**).**

Figure 6. Third mode of variation without height normalization. This mode of variation corresponds to artifacts that are due to the misalignment.

Figure 7. The fourth mode of variation without height normalization. This mode reflects a posture variation. The posture is varying from bending forward to leaning backward.

5.1.3   Third mode

The third mode of variation does not seem to correspond to any anatomical variation. It is rather an artifact that is due to the misalignment in the upper body (Figure 6).

5.1.4   Fourth mode

The fourth mode of variation corresponds to a posture variation (Figure 7). The models vary from a posture that the persons bend forward to a posture that they lean slightly backward.

5.1.5   Fifth mode

The fifth mode of variation represents a difference of muscularity and distribution of mass between the torso and the legs (Figure 8). From one side of the component, models have a large abdomen, narrow hips, and close together thighs. When the correlation to the fifth mode increases, the models tend to become more muscular with larger hips and farther apart thighs. This mode of variation is compa-
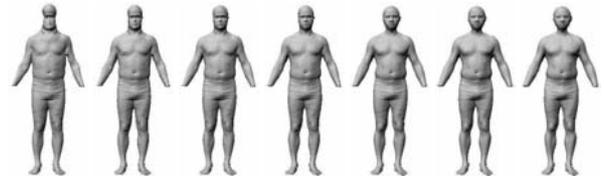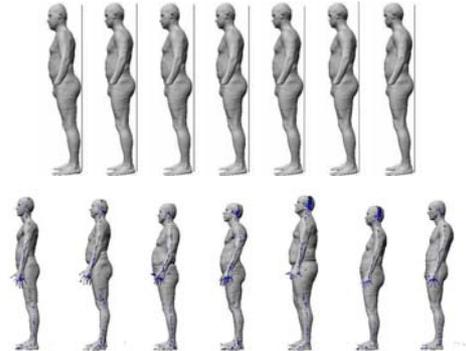
rable to the ectomorph component of the Sheldon representation [17] .

5.2   Normalized models

The application of PCA to the volumetric representation of non-normalized models extracts modes such as the variation of height, weight, posture, and muscularity. However the misalignment between the models generate artifacts as we have seen in the third component. Normalizing the height of the models to the same value reduces the misalignment in the upper body and thus improves the correspondence provided by the volumetric representation.

5.2.1   First mode

Not surprisingly, after normalizing height, the first mode of variation is weight. Showing in Figure 10, this mode of variation, representing 33.86% of the global variability, is equivalent to the second component for the non-normalized models. Notice that the models change from wide to thin as we increase the coefficients whereas in the non-normalized situation (Figure 5), the direction of change is from thin to
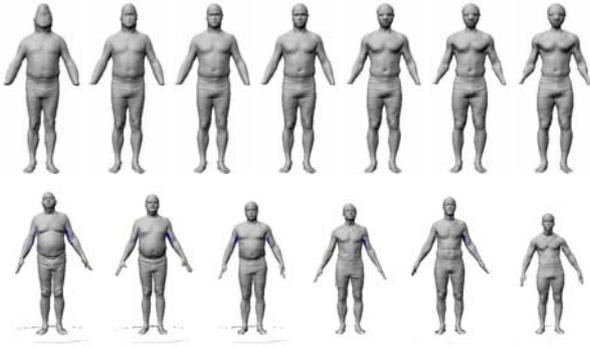
Figure 8. Fifth mode of variation without height normalization. This mode reflects a variation of muscularity and a distribution of mass between the torso and the legs.
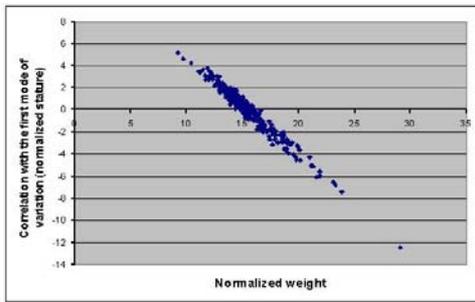

Figure 9. Correlation between the first mode of variation and the normalized weight.

Figure 10. First mode of variation for normalized models. This mode reflects the weight variation representing 34% of the global variability.

Figure 11. Second mode of variation with height normalization

wide. This is because the direction of the eigenvectors can be both ways.

The correlation of this mode with the normalized weight is illustrated in the Figure 9.

5.2.2 Second mode

The second mode of variation is equivalent to the fourth mode of variation in the non-normalized models. It reflects a posture variation where the models are bending forward on the one side and leaning backward on the other (Figure 11). This mode of variation represents 15.11% of the global variability.

5.2.3 Third mode

The third mode of variation represents 8.93% of the global variability. This component corresponds to a variation of mass distribution and muscularity (Figure 13). It is equivalent to the fifth mode in the non-normalized models. Figure 12 illustrates a correlation between this mode and the
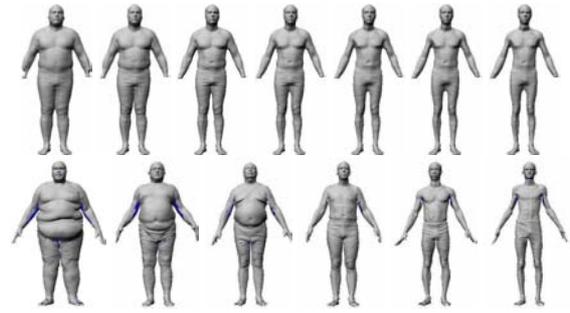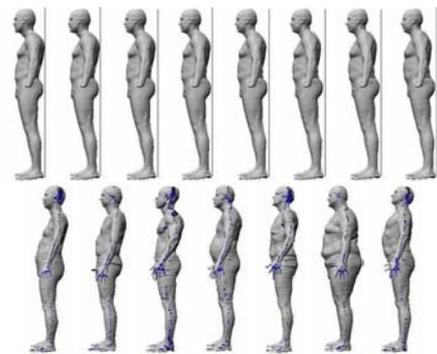
waist / hip circumference ratio. We notice that for low correlation coefficients, the waist circumference is larger than the hip circumference, whereas for high coefficients the hips are larger.

5.2.4 Fourth mode

The fourth mode of variation represents 4% of the global variability. It reflects a variation of the spacing between the arms and the torso. In addition, this mode also corresponds to the proportional lengths between the upper and lower body. From Figure 14, we observe that the legs of the models become longer as we increase the correlation coefficient.

5.2.5 Fifth mode

The fifth mode represents 3.64% of the global variation. It corresponds to a variation of the head position relative to the rest of the body. When the head is leaning backward, the back of model tends to have an arch (Figure 15).
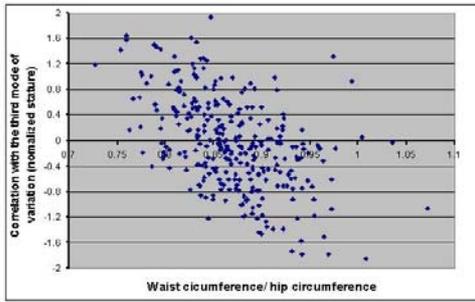
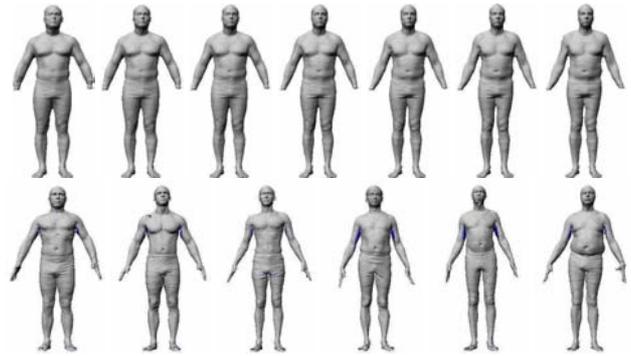**Figure 12. Correlation between the third mode of variation and the waist / hip circumference ratio.**

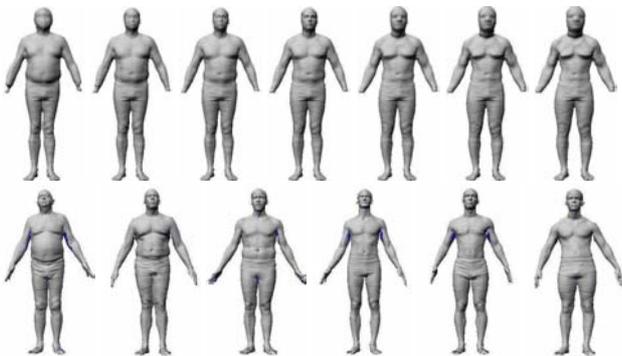**Figure 13. Third mode of variation (normalized)**

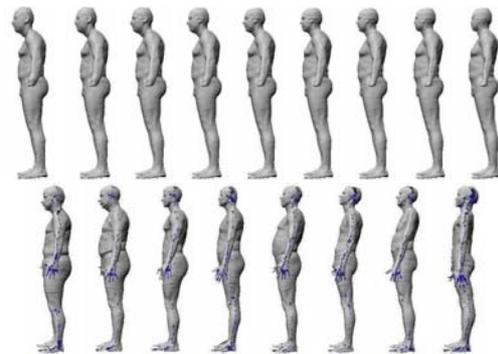**Figure 14. Fourth mode of variation (normalized)**

Figure 15. Fifth mode of variation (normalized)

5.3 Models with segmented arms

The first five modes extracted from the models with segmented arms are similar to the ones extracted in the previous experiment, except for the variation corresponding to the arms (Figure 16). However, the percentages of variability associated to these modes are slightly different from the previous ones. The first five modes of variation represents 36.15%, 9.5%, 6.29%, 5.26%, and 4.61% of the total variability.

6 Conclusions

This paper introduces a new approach to anthropometric measurement based on 3-D scanning technology. Using the distance functions computed on the volumetric representation of 3-D models, we have shown that an extensive human body shape analysis can be performed by principal component analysis without the knowledge of the anatomical landmarks. We applied PCA to 300 male subjects from the CAESAR database to extract the main modes of varia-

tion of the human body shape. In particular, we have shown that the human body shape can be globally represented with a small number of principal components. Furthermore, we have found that the first few components represent meaningful intuitive body variations. We have given interpretations to the first five components—some of them provide quantitative evidence to the empirical anthropometric observations [17].

Our interpretations have yet to be validated by the experts in the fields of anthropometry, anatomy, and anthropology. Nevertheless, this new approach provides powerful tools for these fields and our study is only the first step toward a fast and more reliable characterization of the whole human body.

References

[1] B. Allen, B. Curless, and Z. Popović. The Space of Human Body Shapes: Reconstruction and Parametrisation from Range Scans. *ACM Transactions on Graphics (ACM SIGGRAPH'2003)*, 22(3):587–594, 2003.
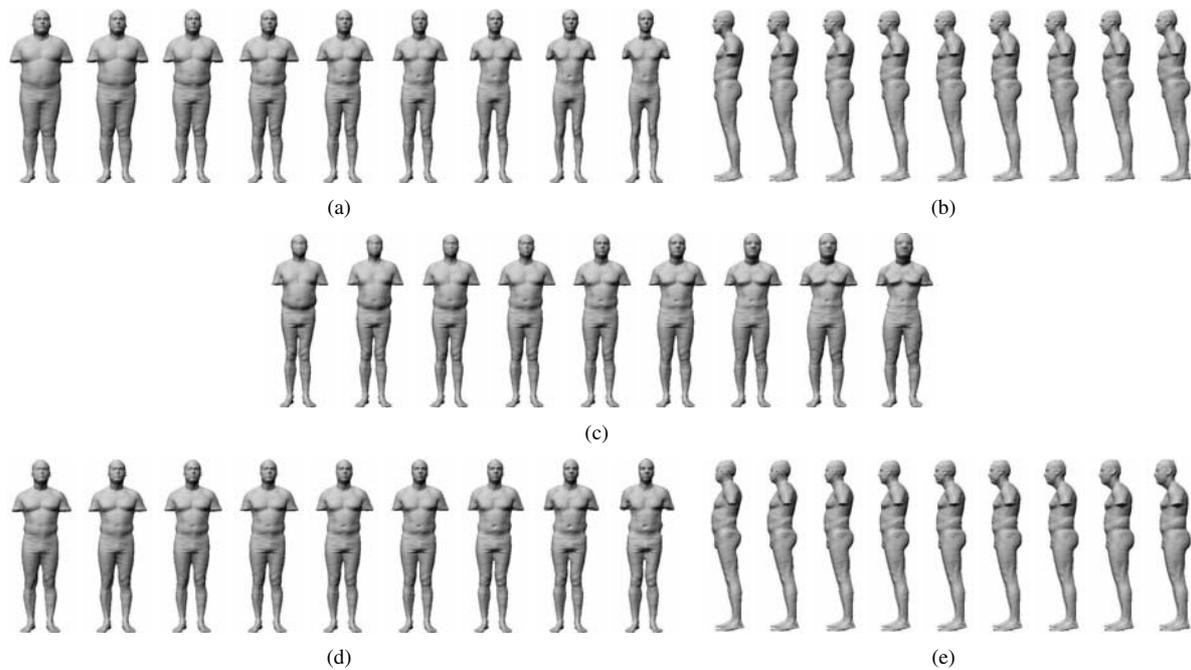
Figure 16. The first five modes of variation after eliminating the arms.

[2] Z. B. Azouz, M. Rioux, and R. Lepage. 3D Description of the Human Body Shape: Application of Karhunen-Love Expansion to the CAESAR database. In *Proceedings of the 16th International Congress and Exibition of Computer Assited Radiology and Surgery*, pages 571–576, Paris, France, June 2002.

[3] Z. B. Azouz, M. Rioux, C. Shu, and R. Lepage. Analysis of human shape variation using volumetric techniques. In *Proc. of 17th Annual Conference on Computer Animation and Social Agents (CASA2004)*, pages 197–206, Geneva, Switzerland, July 2004.

[4] V. Blanz and T. Vetter. A morphable model for the synthesis of 3D faces. In *Proc. of ACM SIGGRAPH 99*, pages 187–194, 1999.

[5] D. Burnsides, M. BoehmerK, and K. Robinette. 3-D Landmark Detection and Identification in the Caesar Project. In *Proceedings of the Third International Conference on 3-D Digital Imaging and Modeling (3DIM'2001)*, pages 393–398, Quebec City, Canada, May 2001.

[6] J. Carr, R. Beatson, J. Cherrie, T. Mitchell, W. Fright, B. Mc-Callum, and T. Evans. Reconstuction and Representation of 3D Objects with Radial Basis Functions. In *Proceedings of ACM SIGGRAPH 2001*, pages 67–76, 2001.

[7] J. Davis, S. Marschner, M. Garr, and M. Levoy. Filling Holes in Complex Surfaces Using Volumetric Diffusion. In *Proceedings of the First International Symposium on 3D Data Processing, Visualization and Transmission*, Padua, Italy, June 2002.

[8] C. Inc. http://www.cyberware.com.

[9] V. Inc. http://www.vitronic.com.

[10] M. Jones. The Production of Volume Data from Triangular Meshes Using Voxelization. *Computer Graphics Forum*, 15(5):311–318, 1996.

[11] A. Kaufman. An Algorithm for 3D Scan Conversion of Polygons. In *Proceedings of EUROGRAPHICS'87*, pages 197–208, Amsterdam, North Holland, August 1987.

[12] A. Kaufman. *Volume Visualization (Tutorial)*. IEEE computer Society Press, 1991.

[13] M. Kirby and L. Sirovich. Application of the Karhunen-Loeve Procedure for the Characterisation of Human Faces. *IEEE Transactions on Pattern Analysis and Machine Intelligence*, 12(1):103–108, 1990.

[14] W. Lorenson and H. Cline. Marching Cubes: A High Resolution 3-D Surface Construction Algorithm. *Proc. SIGGRAPH 1987*, 21(3):163–169, July 1987.

[15] K. Robinette, H. Daanen, and E. paquet. The CAESAR Project: A 3-D Surface Anthropometry Survey. In *Second International Conference on 3-D Digital Imaging and Modeling (3DIM'99*, pages 380–386, Ottawa, Canada, October 1999.

[16] H. Seo and N. Magnenat-Thalmann. An Automatic Modeling of Human Bodies from Sizing Parameters. *SIGGRAPH Symposium on Interactive 3D Graphics*, pages 19–26, July 2003.

[17] W. Sheldon, S. Stevens, and W. Tucker. *The Varieties of Human Physique*. Harper and Brothers Publishers, New York, 1940.

[18] M. Stralen, H. Daanen, and J. Tangelder. A Tool Box to Identify Holes in 3D Human Body Scans. In *Proceedings of the 15th Triennial Congress of the International Ergonomics Association (IEA 2003)*, Seoul, Korea, August 2003.